Electric field manipulation of magnetization at room temperature in multiferroic $CoFe_2O_4/Pb(Mg_{1/3}Nb_{2/3})_{0.7}Ti_{0.3}O_3$ heterostructures

J. J. Yang,[1] Y. G. Zhao,[1,a)] H. F. Tian,[1] L. B. Luo,[1] H. Y. Zhang,[1] Y. J. He,[1] and H. S. Luo[2]
[1]*Department of Physics and State Key Laboratory of New Ceramics and Fine Processing, Tsinghua University, Beijing 100084, People's Republic of China*
[2]*State Key Laboratory of High Performance Ceramics and Superfine Microstructure, Shanghai Institute of Ceramics, Chinese Academy of Sciences, Shanghai 201800, People's Republic of China*

(Received 16 March 2009; accepted 6 May 2009; published online 27 May 2009)

Multiferroic heterostructures were fabricated by growing ferrimagnetic $CoFe_2O_4$ films on ferroelectric $Pb(Mg_{1/3}Nb_{2/3})_{0.7}Ti_{0.3}O_3$ substrates using pulsed laser deposition. Upon applying an electric field, the in-plane magnetization of the heterostructures increases and the out-of-plane magnetization decreases. Sharp and reversible changes in magnetization under electric field were also observed for the poled sample. The relative change in magnetization-electric field hysteresis loops were obtained for both the in-plane and out-of-plane magnetizations. Analysis of the results suggests that the electric field induced change in magnetic anisotropy via strain plays an important role in the magnetoelectric coupling in the heterostructures.
[DOI: 10.1063/1.3143622]

Multiferroic materials with magnetoelectric (ME) coupling have attracted much attention due to their interesting properties and potential applications.[1–7] Because single-phase multiferroic materials are rare, ferromagnetic/ferroelectric (FM/FE) heterostructures with FM thin films grown on FE substrates provide an alternative way for exploring ME effect via accurately controlled interface.[8,9] In these studies, one of the key issues is the manipulation of magnetism of FM/FE heterostructures by electric field and the work on this aspect is still limited. Eerenstein *et al.*[8] reported on an electric field induced sharp and nonreversible decrease in magnetization in $La_{0.67}Sr_{0.33}MnO_3/BaTiO_3$ heterostructure and attributed this effect to the change in magnetic anisotropy induced by the electric-field-controlled strain. Thiele *et al.*[9] also showed that an electric field can lead to magnetization change in the perovskite manganites/FE heterostructure and they proposed that the changes in saturation magnetization and Curie temperature of manganite induced by the electric-field-controlled strain are essential. The spinel $CoFe_2O_4$ (CFO) is a predominant ferrimagnetic material with a large magnetostriction and high Curie temperature (840 K for thin films).[10–12] On the other hand, $Pb(Mg_{1/3}Nb_{2/3})_{0.7}Ti_{0.3}O_3$ (PMN-PT) single crystal is a well-known relaxor FE material with excellent piezoelectric activity.[13] So, the heterostructures of CFO/PMN-PT is a good candidate for the study of ME coupling effect. However, there have been no reports on CFO/PMN-PT heterostructure. In this letter, we report on the electric field manipulation of magnetization at room temperature in CFO/PMN-PT heterostructures. The results suggest that the electric field induced change in magnetic anisotropy via strain plays an important role in the manipulation of magnetization.

CFO films were deposited on the one-side-polished $3\times3\times0.6$ mm^3 (001) PMN-PT substrates by pulsed laser deposition (KrF excimer laser, $\lambda=248$ nm). During deposition, the temperature of the substrate was kept at 670 °C and the oxygen pressure was 4 Pa. The laser energy density was approximately 2 J/cm^2 with a repetition rate of 5 Hz. After deposition, the films were furnace cooled to room temperature in an oxygen atmosphere of 4 Pa. The film thickness is about 200 nm. X-ray diffraction of CFO/PMN-PT was performed using a Rigaku D/max-RB x-ray diffractometer with a Cu $K\alpha$ radiation and the result is shown in Fig. 1(a), which indicates that CFO film is (004) orientated. The out-of-plane lattice parameter was calculated to be 0.839 nm. Silver paint was used as the electrical contact for CFO/PMN-PT and it covered the full area of the film and the back of PMN-PT. The silver paint in contact with CFO is defined as the positive electrode. The magnetic property was measured with a superconducting quantum interference device (MPMS 7T, Quantum Design). The voltage was applied *in situ* on the sample by an electrometer (model 6517A, Keithley) during the magnetic measurement. The polarization–electric field (P-E) loops of the samples were measured using a Radiant Technologies Precision Premier II system.

Figure 1(b) shows the in-plane and out-of-plane magnetic hysteresis loops for CFO films. Considering the shape anisotropy, the demagnetizing field has been subtracted for the out-of-plane data. It can be seen that a small magnetic anisotropy exists with the out-of-plane direction as the mag-

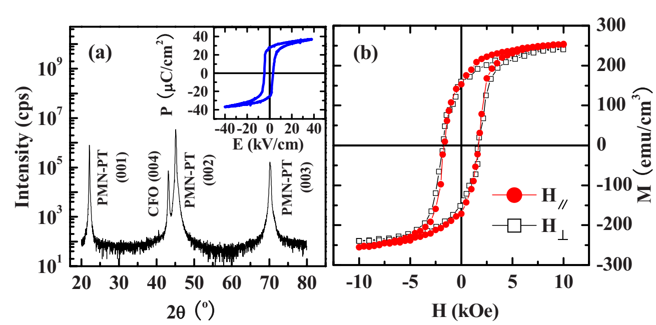

FIG. 1. (Color online) (a) XRD pattern for CFO/PMN-PT. The inset is the P-E loop of PMN-PT. (b) In-plane ($H_{\parallel}$) and out-of-plane ($H_{\perp}$) magnetic hysteresis loops for CFO/PMN-PT.

a)Electronic mail: ygzhao@tsinghua.edu.cn.

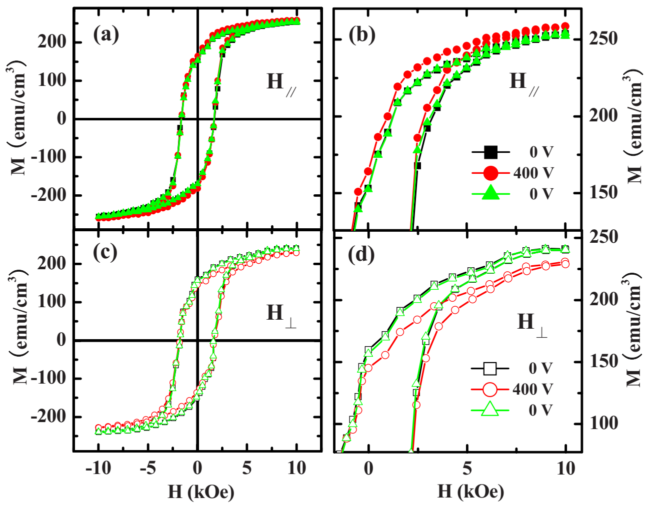

FIG. 2. (Color online) (a) In-plane magnetic hysteresis loops under 0 V (square), 400 V (circle), and 0 V after removal of 400 V (triangle). (b) Expanded view of the first quadrant of (a). (c) Out-of-plane magnetic hysteresis loops under 0 V (square), 400 V (circle), and 0 V after removal of 400 V (triangle). (d) Expanded view of the first quadrant of (c).

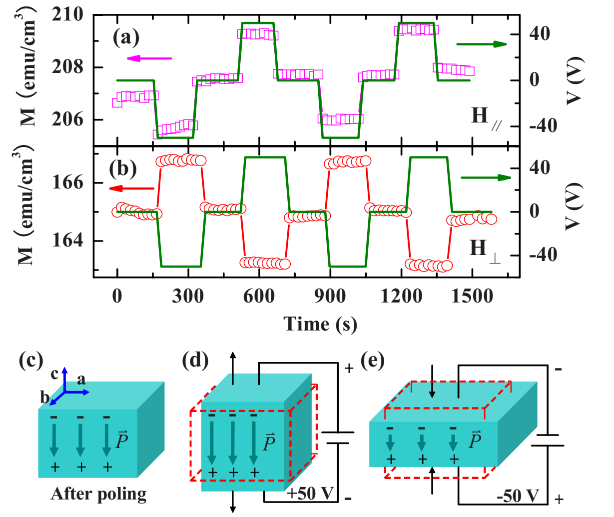

FIG. 3. (Color online) (a) In-plane magnetization (left axis, open square) and the applied electric field (right axis, line) as a function of time, the magnetic field is 0.05 T. (b) Out-of-plane magnetization (left axis, open circle) and the applied electric field (right axis, line) as a function of time, the magnetic field is 0.2 T. (c) The definition of coordinate system and the polarization of PMN-PT after poling with a +400 V voltage. (d) Application of a +50 V voltage to the positively polarized PMN-PT. (e) Application of a −50 V voltage to the positively polarized PMN-PT. The dashed lines in (d) and (e) show the shape of the sample as given in (c).

netic hard direction. This is likely due to the in-plane compressive strain of PMN-PT since it has been shown that CFO thin films under compressive strain have an out-of-plane magnetic hard direction.[12] The bulk CFO has a cubic unit cell with lattice parameters of 0.838 nm. The in-plane lattice parameters of PMN-PT are $a=b=0.4022$ nm, which are smaller than half of the CFO lattice parameters. Hence, the CFO films grown on PMN-PT are under biaxial compressive strain. This is consistent with the increase in the out-of-plane lattice parameter of CFO films obtained from Fig. 1(a). Because our CFO films are thick (200 nm), the in-plane compressive strain is partially relaxed, as shown by the shift in the x-ray diffraction peaks with film thickness (not shown here). Thus, the magnetic anisotropy of CFO associated with the in-plane compressive strain is not large. The *P-E* loop of the PMN-PT substrate without CFO films is shown in the inset of Fig. 1(a), which indicates that the coercive field of PMN-PT is +3.2 kV/cm for the positive electric field and −4.6 kV/cm for the negative electric field. The asymmetry of the coercive fields may originate from the internal field in the PMN-PT crystal as observed in the $LiTaO_3$ single crystal.[14]

In order to investigate the electric field manipulation of magnetization, we measured the in-plane and out-of-plane magnetic hysteresis loops under the voltages of 0 V, +400 V (6.67 kV/cm), and 0 V (after removal of the +400 V voltage). The in-plane magnetic hysteresis loops are plotted in Fig. 2(a) and the details of the first quadrant are shown in Fig. 2(b). They show that the in-plane magnetization increases under electric field and restores to its initial values after removal of the electric field. Figure 2(c) is the out-of-plane magnetic hysteresis loops and Fig. 2(d) gives the details of the first quadrant. The out-of-plane magnetization decreases under electric field and restores to its initial states after removal of the electric field. Similar behavior is present in the third quadrant of Figs. 2(a) and 2(c). The manipulation of magnetization by electric field can be understood by considering the electric-field-controlled strain which results in the change in the magnetic anisotropy. The in-plane stress anisotropy energy can be described by $E=K_{me}\cos^2\theta$, where $\cos\theta$ is the directional cosine of the magnetization vector along the film normal.[10] K_{me} is the anisotropy constant associated with stress and $K_{me}=-3\lambda_{100}\sigma_{100}/2$, where $\lambda_{100}(-350\times10^{-6})$ is the in-plane magnetostriction coefficient of CFO films and σ_{100} is the in-plane stress of CFO films.[10,11] In the CFO/PMN-PT heterostructures, CFO films are under compression, i.e., $\sigma_{100}<0$, which results in $K_{me}>0$. So the energy for the out-of-plane direction is higher than that of the in-plane direction, which is consistent with the results shown in Fig. 1(b). The electric field applied along (001) direction leads to the elongation of the lattice parameter for PMN-PT along (001) direction through the converse piezoelectric effect and thus enhances σ_{100}, resulting in an increase in K_{me}. As a result, the in-plane magnetization increases and the out-of-plane magnetization decreases under electric field.

Since electric field can manipulate the magnetization of CFO in the CFO/PMN-PT heterostructures, we also studied the manipulation of magnetization of CFO in the CFO/PMN-PT by electric voltages with different polarities. First, PMN-PT in the CFO/PMN-PT heterostructure was poled by applying a voltage of +400 V (6.67 kV/cm, exceeding the coercive field) so that it is in a positively polarized state. Then the magnetization of CFO/PMN-PT was measured as a function of time with the electric voltages of ±50 V (0.83 kV/cm) switching on and off alternately. Figure 3(a) shows the in-plane magnetization measured with a magnetic field of 0.05 T. The magnetization decreases sharply when a −50 V voltage is switched on and rapidly returns to its initial state after removal of the voltage. In contrast, the magnetization increases sharply when a +50 V voltage is switched on and also rapidly returns to its initial state after removal of the voltage. The magnitude of ΔM is approximate 1.67 emu/cm^3 for both −50 and +50 V voltages. ΔM is defined as $\Delta M=M(E)-M(0)$, where $M(E)$ is the magnetization under electric field and $M(0)$ is the magnetization under zero electric field. Figure 3(b) shows the out-of-plane mag-

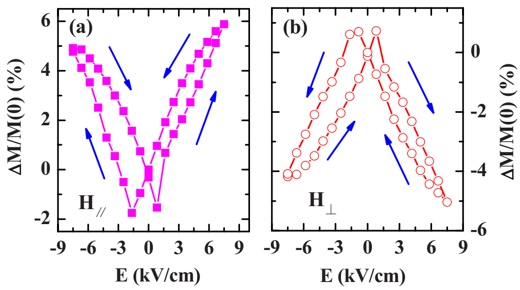

FIG. 4. (Color online) (a) In-plane $\Delta M/M(0)-E$ loop, the magnetic field is 0.05 T. (b) Out-of-plane $\Delta M/M(0)-E$ loop, the magnetic field is 0.2 T.

netization measured with a magnetic field of 0.2 T. The magnetization increases under a −50 V voltage and decreases under a +50 V voltage, which is opposite to that shown in Fig. 3(a). The magnitude of ΔM is also about 1.67 emu/cm^3 for both −50 and +50 V voltages. These results can be understood as follows. Figure 3(c) illuminates the defined coordinate system and the polarization of PMN-PT after poling with a +400 V voltage. Figure 3(d) shows that the PMN-PT expands along *c* axis with application of a +50 V voltage, resulting in an enhancement in the in-plane compression, which increases the in-plane magnetization and decreases the out-of-plane magnetization. When the +50 V voltage is switched off, PMN-PT rapidly returns to its initial polarized state, leading to the return of magnetization to its initial value. In contrast, Fig. 3(e) shows that the PMN-PT contracts along *c* axis with application of a −50 V voltage, resulting in a decrease in the in-plane compression, which decreases the in-plane magnetization and increases the out-of-plane magnetization. If PMN-PT is poled with a −400 V voltage, the magnetization can also be tuned by controlling the polarization states of PMN-PT with opposite effect compared to that of the +400 V polarized states (not shown here). A similar picture has been used to explain the electric field induced resistance change via strain in the manganite/PMN-PT heterostructures.[15]

We also measured the relative change in magnetization $[\Delta M/M(0)]$-electric field(E) loops. The sample had been magnetized by a magnetic field of 1 T before the measurement. Figure 4(a) shows the in-plane $\Delta M/M(0)-E$ loops measured with a magnetic field of 0.05 T. It can be seen that the loop has a butterfly shape, which agrees with the strain-electric field loop of PMN-PT.[16] Figure 4(b) shows the out-of-plane $\Delta M/M(0)-E$ loop measured with a magnetic field of 0.2 T. It also has a butterfly shape but is opposite to the in-plane loop shown in Fig. 4(a). The maximum of in-plane $\Delta M/M(0)$ is 6%, which is approximately equal to the out-of-plane value (5%). The in-plane $\Delta M/M(0)$ estimated from Fig. 4(a) changes between −2% and 6%, corresponding to change in magnetization from 192.8 to 228.3 emu/cm^3. These magnetizations are in the upper branch of *M*-*H* loop shown in Fig. 2(b), which corresponds to the reversible process of magnetization. Hence, the hysteresis in Fig. 4(a) is likely due to the hysteresis of strain-electric field loop in PMN-PT.[16] This scenario also applies to the out-of-plane case [Fig. 4(b)]. In addition, the electric fields of the minimum magnetization in Fig. 4(a) are $E^+_{\min}\sim+0.83$ kV/cm for the positive electric field and $E^-_{\min}\sim-1.67$ kV/cm for the negative electric field, which are much smaller than those obtained from the *P*-*E* loop in the inset of Fig. 1(a). This can be understood since the switching of the FE domains begins at the interface under electric field lower than the coercive field,[17] while the effect of strain on CFO originates at the interface. The asymmetry between $E^+_{\min}$ and $E^-_{\min}$ is consistent with the asymmetry of the coercive fields shown in the inset of Fig. 1(a). The maximal *ME* coupling coefficient $\alpha=\mu_0 dM/dE$ is 3.2×10^{-8} s m^{-1}, as derived from Fig. 4(a), with $E=1.67$ kV/cm. The sharp and reversible α derived from Fig. 3 is 2.5×10^{-8} s m^{-1}. These values are comparable to that of $CoFe_2O_4$ nanopillars in a $BiFeO_3$ matrix ($\sim10^{-8}$ s m^{-1}).[18]

This work was supported by the 973 project (Grant No. 2009CB929202), National Science Foundation of China (Grant Nos. 50872065 and 10674079), and Tsinghua National Laboratory for Information Science and Technology (TNList) Cross-discipline Foundation.

[1]M. Fiebig, J. Phys. D: Appl. Phys. **38**, R123 (2005).
[2]W. Prellier, M. P. Singh, and P. Murugavel, J. Phys.: Condens. Matter **17**, R803 (2005).
[3]W. Eerenstein, N. D. Mathur, and J. F. Scott, Nature (London) **442**, 759 (2006).
[4]R. Ramesh and N. A. Spaldin, Nature Mater. **6**, 21 (2007).
[5]S. W. Cheong and M. Mostovoy, Nature Mater. **6**, 13 (2007).
[6]C.-W. Nan, M. I. Bichurin, S. Dong, D. Viehland, and G. Srinivasan, J. Appl. Phys. **103**, 031101 (2008).
[7]Y. Tokura, Science **312**, 1481 (2006).
[8]W. Eerenstein, M. Wiora, J. L. Prieto, J. F. Scott, and N. D. Mathur, Nature Mater. **6**, 348 (2007).
[9]C. Thiele, K. Dörr, O. Bilani, J. Rödel, and L. Schultz, Phys. Rev. B **75**, 054408 (2007).
[10]S. Chikazumi, *Physics of Magnetism* (Wiley, New York, 1984).
[11]H. Zheng, J. Wang, S. E. Lofland, Z. Ma, L. Mohaddes-Ardabili, T. Zhao, L. Salamanca-Riba, S. R. Shinde, S. B. Ogale, F. Bai, D. Viehland, Y. Jia, D. G. Schlom, M. Wuttig, A. Roytburd, and R. Ramesh, Science **303**, 661 (2004).
[12]Y. Suzuki, G. Hu, R. B. von Dover, and R. J. Cava, J. Magn. Magn. Mater. **191**, 1 (1999).
[13]H. Cao, V. H. Schmidt, R. Zhang, W. W. Cao, and H. S. Luo, J. Appl. Phys. **96**, 549 (2004).
[14]V. Gopalan and M. C. Gupta, Appl. Phys. Lett. **68**, 888 (1996).
[15]R. K. Zheng, Y. Wang, J. Wang, K. S. Wong, H. L. W. Chan, C. L. Choy, and H. S. Luo, Phys. Rev. B **74**, 094427 (2006).
[16]Z. Feng, D. Lin, H. Luo, S. Li, and D. Fang, J. Appl. Phys. **97**, 024103 (2005).
[17]M. Dawber, K. M. Rabe, and J. F. Scott, Rev. Mod. Phys. **77**, 1083 (2005).
[18]F. Zavaliche, H. Zheng, L. Mohaddes-Ardabili, S. Y. Yang, Q. Zhan, P. Shafer, E. Reilly, R. Chopdekar, Y. Jia, P. Wright, D. G. Schlom, Y. Suzuki, and R. Ramesh, Nano Lett. **5**, 1793 (2005).